Effects of Conditioning Depolarization and Repetitive Stimulation on Q_β and Q_γ Charge Components in Frog Cut Twitch Fibers

CHIU SHUEN HUI and WEI CHEN

From the Department of Physiology and Biophysics, Indiana University Medical Center, Indianapolis, Indiana 46202

ABSTRACT Charge movement was measured in frog cut twitch fibers with the double Vaseline-gap technique. Steady-state inactivation of charge movement was studied by changing the holding potential from −90 mV to a level ranging from −70 to −30 mV. Q_β and Q_γ at each holding potential were separated by fitting the *Q-V* plot with a sum of two Boltzmann distribution functions. At −70 mV Q_β and Q_γ were inactivated to 54.0% (SEM 2.2) and 82.7% (SEM 3.0) of the amounts at −90 mV. At holding potentials ≥ −60 mV, more Q_γ was inactivated than Q_β, and at −30 mV Q_γ was completely inactivated but Q_β was not. There was no holding potential at which Q_β was unaffected and Q_γ was completely inactivated. The differences between the residual fractions of Q_β and Q_γ are significant at all holding potentials ($P < 0.001$–0.05). The plot of the residual fraction of Q_β or Q_γ versus holding potential can be fitted well by an inverted sigmoidal curve that is a mirror image of the activation curve of the respective charge component. The pair of curves for Q_γ correlates well with those for tension generation or Ca release obtained by other investigators. The time courses of the inactivation of Q_β and Q_γ were studied by obtaining several *Q-V* plots with conditioning depolarizations lasting 1–20 s and separating each *Q-V* plot into Q_β and Q_γ components by fitting with a sum of two Boltzmann distribution functions. The inactivation time constant of Q_β was found to be 5–10 times as large as that of Q_γ. During repetitive stimulation, prominent I_γ humps could be observed in TEST-minus-CONTROL current traces and normal Q_γ components could be separated from the *Q-V* plots, whether 20 or 50 mM EGTA was present in the internal solution, whether 2 or 10 stimulations were used, and whether the stimuli were separated by 400 ms or 6 s. Repetitive stimulation slowed the kinetics of the I_γ hump and could shift the *Q-V* curve slightly in the depolarizing direction in some cases, resulting in an apparent suppression of charge at the potentials that fall on the steep part of the *Q-V* curve.

Address reprint requests to Dr. Chiu Shuen Hui, Department of Physiology and Biophysics, Indiana University Medical Center, 635 Barnhill Drive, Indianapolis, IN 46202.

Dr. Chen's present address is Department of Surgery, University of Chicago, 5841 S. Maryland Ave., Chicago, IL 60637.

J. GEN. PHYSIOL. © The Rockefeller University Press · 0022-1295/92/06/1017/27 $2.00
Volume 99 June 1992 1017–1043

INTRODUCTION

The preceding paper (Hui and Chen, 1992) shows that 0.5–1.0 mM tetracaine can be used to dissect out a steeply voltage-dependent charge component from the charge versus voltage (Q-V) plots of the total charge measured from cut fibers, referred to as method 1. The results agree qualitatively with those obtained from intact fibers (Hui, 1983*a*, *b*), although the dose–response relationships of the effect differ quantitatively in the two preparations. The steeply voltage-dependent component dissected with the pharmacological approach agrees well with the components separated by three other existing, independent methods: method 2 (in intact fibers: Hui, 1983*a*; in cut fibers: Hui, 1991*a*), method 3 (in cut fibers: Hui and Chandler, 1990; in intact fibers: Hui, 1991*a*), and method 4 (in cut fibers: Hui and Chandler, 1991).

Originally, Adrian and Peres (1979) separated Q_β and Q_γ in intact fibers by changing the holding potential and making use of the difference in steepness between the steady-state inactivation of the two components. They assumed that when the holding potential was set at −40 mV, Q_β was completely mobile and Q_γ was completely inactivated. Hui (1983*b*) found some inconsistency between the amounts of Q_γ in intact fibers separated by their method and by method 2. Because of the inherent difficulties in measuring charge movement in intact fibers with the three-microelectrode technique, the inactivation curves for Q_β and Q_γ obtained from intact fibers could be subjected to substantial uncertainties. With growing interest in the possibility that Q_γ might be the trigger for Ca release from the sarcoplasmic reticulum (SR) (Almers, 1978; Huang, 1982; Hui, 1983*b*, 1991*a*; Vergara and Caputo, 1983; Hui and Chandler, 1990, 1991), it is of interest to study the inactivation curves for Q_β and Q_γ in greater detail and to investigate whether there exists a holding potential at which Q_β and Q_γ can be separated entirely. Another aim of this work is to separate the inactivation time courses of Q_β and Q_γ and see if they are different.

In contrast to the "trigger hypothesis" for Q_γ, a "feedback hypothesis" has also been proposed. In the latter hypothesis, Q_γ arises as a result of Ca release, as suggested originally by Dr. Knox Chandler (see Discussions sections in Horowicz and Schneider, 1981, and in Hui, 1983*b*). One piece of evidence that might be consistent with the feedback hypothesis was provided by Garcia et al. (1990), who observed that the I_γ humps in charge movement traces from cut fibers disappeared when the Ca^{2+} released from the SR into the myoplasm was chelated by a high $[EGTA]_i$ and the effect was reversible. To understand the cause of the disappearance of I_γ humps, we loaded cut fibers with different $[EGTA]_i$ and found that substantial I_γ humps still existed during repetitive stimulation.

A preliminary report of some of the findings in this paper has appeared (Chen and Hui, 1989).

METHODS

Solutions

All concentrations are in millimolar.

Relaxing solution. Solution A: 120 K·glutamate, 1 $MgSO_4$, 0.1 K_2·EGTA, and 5 K_2·PIPES, pH 7.0.

Internal solution. Solution B: 45.5 Cs·glutamate, 20 Cs_2·creatine phosphate, 20 Cs_2·EGTA, 6.8 $MgSO_4$, 5.5 Cs_2·ATP, 5 glucose, and 5 Cs_2·PIPES, pH 7.0. Solution C: 20 Cs_2·creatine phosphate, 50 Cs_2·EGTA, 6.8 $MgSO_4$, 5.5 Cs_2·ATP, 5 glucose, and 5 Cs_2·PIPES, pH 7.0.

External solution. Solution D: 120 TEA·Cl, 2.5 RbCl, 1.8 $CaCl_2$, 2.15 Na_2HPO_4, and 0.85 NaH_2PO_4, pH 7.1.

TEA^+ and Rb^+ in solution D and Cs^+ in solutions B and C were used to minimize K^+ currents. 1 μM tetrodotoxin was added to solution D to block Na^+ current. Solutions B and C contained no added Ca, except for the trace amount of Ca present in Cs·glutamate, estimated to be 60 μM.

For muscle and fiber preparation, see the preceding paper (Hui and Chen, 1992).

Pulse Protocol

The procedure for measuring charge movement at a holding potential of −90 mV was described in the preceding paper (Hui and Chen, 1992). For a less negative holding potential, V_H, the pulse protocol was modified, as illustrated in Fig. 1. Panel *A* shows the CONTROL pulse sequence. To compare data at this V_H with those at −90 mV, the fiber was always held at

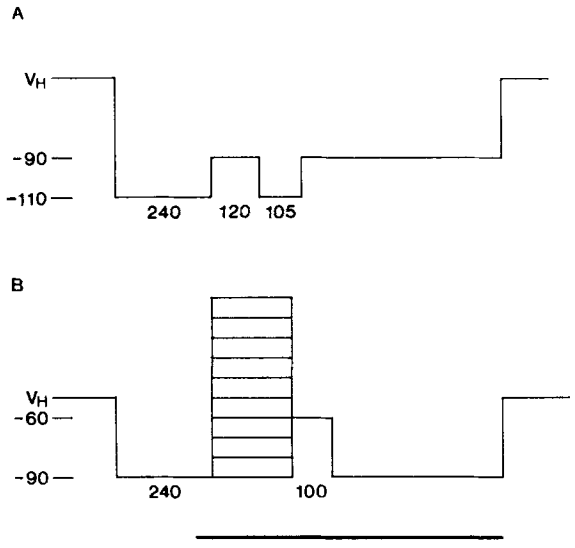

FIGURE 1. Pulse protocol for conditioning depolarization experiments. (*A*) CONTROL pulse. (*B*) TEST pulses. The negative numbers on the left of each panel represent membrane potentials in millivolts. V_H denotes holding potential. The numbers below each trace represent the durations of the intervals in milliseconds. The family of pulses in *B* represents the two-pulse protocol. The one-pulse protocol is achieved by omitting the 100 ms post-pulse. The durations of the TEST pulses vary according to the level of depolarization (see text). The thick horizontal bar at the bottom shows the time period during which the analog signals are sampled.

−110 mV for 240 ms before being stimulated by the CONTROL pulse sequence, consisting of two transitions from −110 to −90 mV, separated by 225 ms. The average of the two ON currents in the signal-averaged CONTROL current trace was used for the subtraction of the linear current components in the single-sweep TEST current trace (see Chandler and Hui, 1990, for the advantage of this protocol).

Fig. 1 *B* shows the TEST pulse sequence for the two-pulse protocol. The one-pulse protocol can be achieved by omitting the 100-ms post-pulse. The fiber was always held at −90 mV for 240 ms before being stimulated by the TEST pulse sequence. For simplicity, all the TEST pulses to different potentials are drawn in the figure with the same duration. In reality, TEST pulse duration decreased with increasing levels of depolarization (Figs. 2, 5, 8, 11, and 14) in order to minimize the activation of nonlinear ionic currents.

Sampling of the three analog signals, V_1, V_2, and I_2, was started 40 ms before the rising edge of the CONTROL or TEST pulse and lasted until the end of the final interval at −90 mV. The

duration of the final interval was adjusted such that the total sampling interval was either 768 or 1,024 ms. Each point in a current trace corresponds to 1 ms.

The two-pulse protocol should be distinguished from another pulse protocol, referred to as the double-pulse protocol. The former protocol consists of a TEST pulse and a post-pulse with no break in between, whereas the latter consists of two identical TEST pulses separated by a repolarization period of 400 ms. In this paper, the latter pulse protocol was always applied from a holding potential of −90 mV.

Data Analysis

The procedures for data analysis were also similar to those used in the preceding paper (Hui and Chen, 1992). For convenience, Eqs. 1–4 in that paper are listed here again. The steady-state Q-V plot obtained with the one-pulse protocol was fitted by a sum of two Boltzmann distribution functions with CONTROL charge correction:

$$Q(V) = \sum_{i=\beta}^{\gamma} Q_{i,\max} F_i^*(V) \tag{1}$$

$$F_i^*(V) = F_i(V) - [F_i(-90) - F_i(-110)](V + 110)/20 - F_i(-110) \tag{2}$$

$$F_i(V) = \left[1 + \exp\left(-\frac{V - \overline{V}_i}{k_i}\right)\right]^{-1} \tag{3}$$

in which $Q_{i,\max}$ represents the maximum amount of charge, $\overline{V}_i$ the equi-distribution potential, and k_i the voltage dependence (or inverse steepness) factor, for $i = \beta$ or γ. Also, the gap correction procedure of Hui and Chandler (1990) was applied. Occasionally, a Q-V plot was fitted by a single Boltzmann distribution function, which is equivalent to dropping one of the two terms on the right-hand side of Eq. 1.

When the two-pulse protocol was used, the Q-V plot of the final OFF charge at −90 mV was fitted by:

$$Q(V) = A + \rho Q_{\gamma,\max}\left[1 + \exp\left(-\frac{V - \overline{V}_i}{k_\gamma}\right)\right]^{-1} \tag{4}$$

with gap correction. A and ρ are constants independent of V and have been expressed explicitly in Hui and Chandler (1991).

In addition, the steady-state inactivation data of Q_β or Q_γ were fitted by the (normalized) inverted sigmoidal function:

$$G_i(V) = \left[1 + \exp\left(\frac{V - \overline{V}_i^*}{k_i^*}\right)\right]^{-1} \tag{5}$$

which is a mirror image of the (normalized) activation curve, Eq. 3 above.

RESULTS

Voltage-dependent Inactivation of Q_β and Q_γ in a Cut Fiber

In the experiment shown in Fig. 2, charge movement was studied with the one-pulse protocol. Panel *A* shows a family of TEST-minus-CONTROL current traces taken at a V_H of −90 mV. The traces resemble those obtained previously under identical conditions (Hui and Chandler, 1990; Hui, 1991*a*, *b*). At potentials ≤ -65 mV only fast I_β transients can be seen in the ON and OFF segments of the traces. At −60 mV

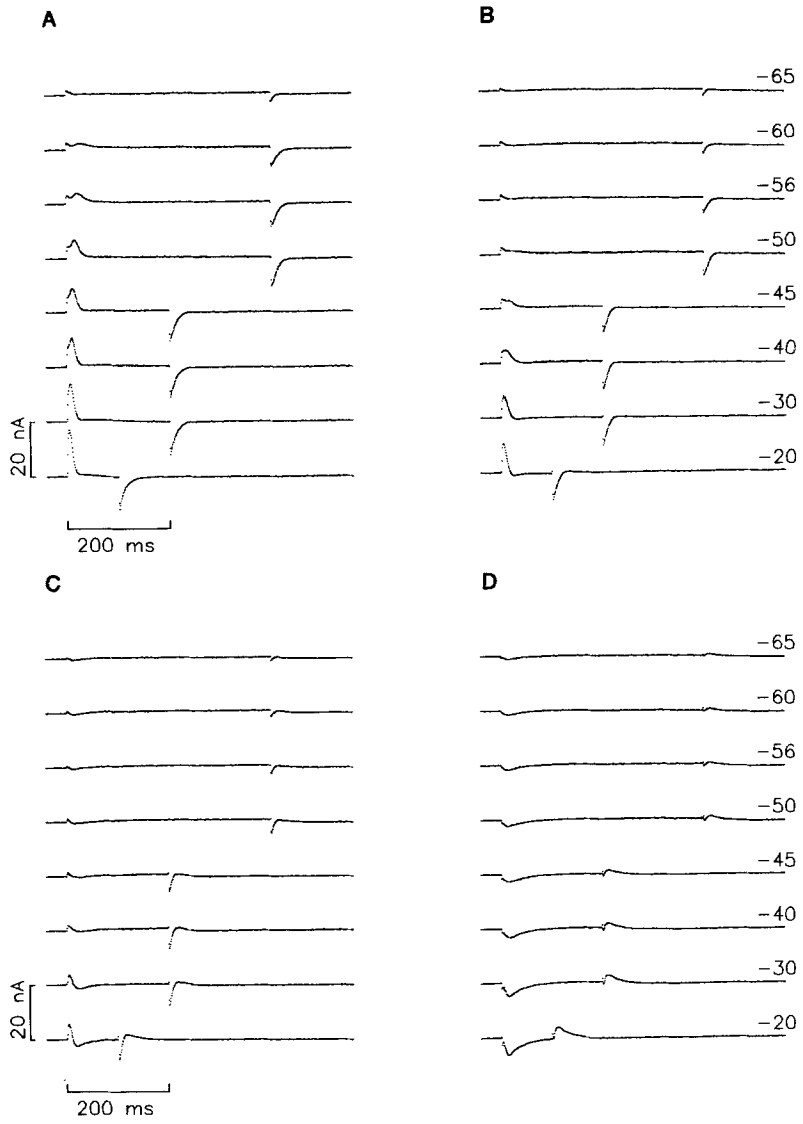

FIGURE 2. Effect of maintained depolarization on TEST-minus-CONTROL current in a cut fiber. Fiber identification: 89021. Diameter = 93 μm. Sarcomere length = 3.5 μm. Saponin treatment was applied to membrane segments in both end pools at time zero. After rinsing, the solutions in the end pools were replaced by solution B. The solution in the center pool was then changed to an isotonic TEA·Cl solution (solution D). At the 21st minute the voltage clamp was turned on and the holding potential was set at −90 mV. From the beginning to the end of the experiment, the holding current (bracketed at −90 mV) changed from −22 to −29 nA and $r_e/(r_e + r_i)$ decreased from 0.989 to 0.988. The one-pulse protocol was used to obtain the traces shown in this figure. (*A*) Traces taken from the 57th to the 76th minute. At the 119th minute the holding potential was changed to −70 mV. (*B*) Traces taken from the 132nd to the 151st minute. At the 180th minute the holding potential was changed to −60 mV. (*C*) Traces taken from the 194th to the 213th minute. At the 242nd minute the holding potential was changed to −50 mV. (*D*) Traces taken from the 256th to the 275th minute. The numbers at the right show the potentials in millivolts during the TEST pulses (the same for both traces in the same row). Only representative traces are shown in each panel.

a broad I_γ hump begins to appear in the ON segment, but not in the OFF segment. At −56 mV the I_γ hump becomes very pronounced. With further depolarizations, the peak amplitude of the I_γ hump increases progressively and rises above the peak of the I_β component. At ≥ -30 mV the hump fuses with, and cannot be visually separated from, the early I_β component.

After changing the V_H to −70 mV, the traces in Fig. 2 *B* were taken. The I_γ humps in the ON segments of Fig. 2 *A* at −60 and −56 mV disappear in Fig. 2 *B*, whereas those at more depolarized potentials are suppressed and their time courses are prolonged. The amplitudes of the OFF transients are also suppressed. The traces in Fig. 2 *C* were taken after the V_H was changed to −60 mV. Both ON and OFF transients are further suppressed and there is no sign of any I_γ hump in the traces. Surprisingly, the ON segments (OFF segments) show an outward (inward) transient followed by a slower inward (outward) transient. These biphasic characteristics of the current transients also exist in the traces of Fig. 2 *B*, but to a lesser extent. At a V_H of −50 mV (Fig. 2 *D*), the fast transients in both ON and OFF segments are greatly

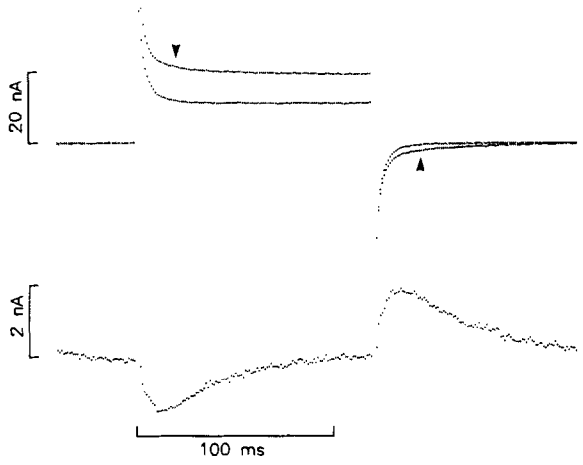

FIGURE 3. Effect of holding potential on the CONTROL current transient. Same fiber as in Fig. 2. The upper pair of superimposed traces shows the CONTROL current traces, one taken when the holding potential was at −90 mV and the other at −40 mV (marked by arrowheads). The difference trace at the bottom was obtained by subtracting the CONTROL trace at −40 mV from that at −90 mV and removing the constant pedestal during the pulse.

suppressed and the slower transients greatly enhanced. This biphasic nature of the current transients has been observed previously by Hui and Milton (1987) in intact fibers and by Hui (1990) in cut fibers in the presence of D600, and also by Chen and Hui (1991*b*) in cut fibers in the presence of nifedipine.

To understand the origin of the biphasic appearance of charge movement, the CONTROL current traces at V_H's of −90 and −40 mV are compared in Fig. 3. In the upper pair of traces, the ON and OFF transients at a V_H of −40 mV show an extra slower component, marked by the arrowheads. A subtraction of the CONTROL current trace at a V_H of −40 mV from that at a V_H of −90 mV yields the lower difference trace. The ON and OFF transients in the difference trace have the same time courses and polarities as the slower ON and OFF transients in the traces of Fig. 2, *C* and *D*.

The origin of the extra slower ON and OFF transients in the CONTROL current trace at a depolarized V_H is not known with certainty. Since the inward and outward deflections in a difference trace are almost symmetrical, they could be capacitive in

nature. A likely candidate for this extra capacitive current is I_α (i.e., Q_α current), which is readily detectable when a fiber is depolarized, as described by Adrian et al. (1976) in intact fibers and Brum and Rios (1987) in cut fibers. When the scaled CONTROL current trace is subtracted from the TEST current trace to generate a TEST-minus-CONTROL current trace at a depolarized V_H, this presumed I_α current gives rise to an inward deflection in the ON segment and an outward deflection in the OFF segment. Moreover, the kinetics of the I_α component appears to be not very voltage dependent and is slower than that of the I_β component, but could be comparable to that of the I_γ component at some potentials.

The ON and OFF transients in the TEST-minus-CONTROL current traces at a V_H of -90 mV (Fig. 2*A*) do not show any biphasicity. If the slower transients of reverse polarity in the other panels of Fig. 2 are indeed caused by I_α current, then it can be concluded that the amount of Q_α is negligible in a normally polarized fiber, consistent with the suggestion given by Hui (1991*b*).

The biphasic nature of the ON and OFF transients in TEST-minus-CONTROL current traces at a V_H of > -90 mV complicates the fitting of baselines to the ON and OFF segments. The slower I_α transient in the OFF segment was removed, although not perfectly ideally, by fitting a sum of an exponential decay and a sloping baseline up to the 70th point or so in that segment (see Fig. 1 of Hui, 1990). No data analysis was performed on the ON segments.

To quantitate the inactivation of Q_β and Q_γ, the amounts of total OFF charge at various V_H's are plotted against TEST pulse potential in Fig. 4. The maximum amount of total charge was progressively reduced when the V_H was changed to a less negative level. Curves 1 and 2 were least-squares fitted to the data at V_H's of -90 and -70 mV, respectively, according to Eq. 1, with gap correction. Curve 1 rises with a shallow slope at the foot and begins to rise steeply at ~ -65 mV due to the activation of Q_γ. The top portion of the curve rises with a shallow slope due to the additional activation of Q_β. Curve 2 represents the Q-V distribution at a V_H of -70 mV. From the values of $q_{\beta,max}/c_m$ and $q_{\gamma,max}/c_m$ listed in the figure legend, it appears that the change in V_H decreased the amounts of Q_β and Q_γ to 44.7 and 67.6% of control, respectively. Thus at a V_H of -70 mV, more Q_β was suppressed than Q_γ in this fiber.

When the Q-V plots at V_H's of -60, -50, and -40 mV were fitted by Eq. 1, the fitting routine did not converge. However, the plots were fitted well by a single Boltzmann distribution function, with CONTROL charge correction and gap correction, represented by curves 3–5. This suggests that probably only one charge component remained mobile at these more depolarized V_H's. Since no I_γ humps can be visualized in the traces of Fig. 2, *C* and *D* (and at a V_H of -40 mV; not shown) and the k values for curves 3–5 are relatively large, it is reasonable to assume that the residual charge at V_H's of -60, -50, or -40 mV belongs to Q_β. However, the value of $q_{\beta,max}/c_m$ for curve 3 is larger than that for curve 2, and the value of k_β for curve 3 is smaller than that for curve 2 (see figure legend), suggesting that there might still be some residual Q_γ at a V_H of -60 mV, but the amount was too small to be resolved by method 3. A remedy will be presented below, in connection with Figs. 5 and 6.

Under the assumption that all the residual charge at a V_H of -50 or -40 mV is totally Q_β, the residual amounts of Q_β were then estimated to be 36.4 and 8.6% of control, respectively, at these levels of V_H. It should be noted that, because of the presence of Q_α, the value of c_m became larger as V_H was changed to a less negative

level (see figure legend). This introduces extra decreases in the values of $q_{\beta,max}/c_m$ and $q_{\gamma,max}/c_m$ in addition to inactivation.

Charge movement was also studied in the same fiber with the two-pulse protocol and the charge components were separated by method 4. Fig. 5 *A* shows TEST-minus-CONTROL current traces taken at a V_H of −90 mV. The ON segments of the traces are identical to those in Fig. 2 *A*, implying that the fiber was stable. After V_H was changed to −70 mV, the ON and OFF transients were suppressed (Fig. 5 *B*). At a V_H of −60 mV the transients were further suppressed (Fig. 5 *C*).

The amounts of OFF charge at various V_H are plotted against TEST pulse potential

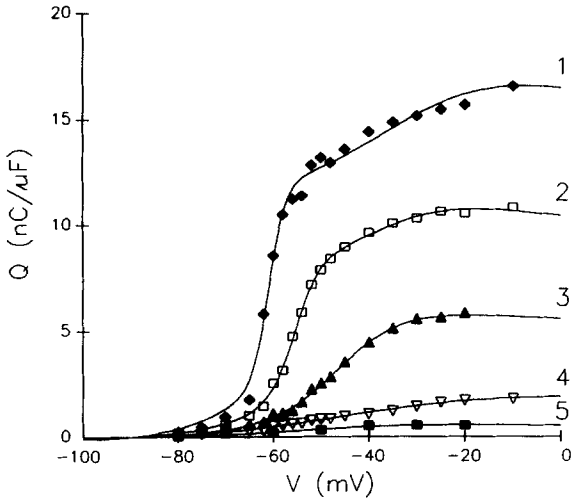

FIGURE 4. Steady-state voltage distributions of Q_β and Q_γ at different holding potentials. Same fiber as in Fig. 2. ◆'s, □'s, ▲'s, ▽'s, and ■'s show data taken at a holding potential of −90, −70, −60, −50, and −40 mV, respectively. The points were obtained from time integrals of OFF current transients in TEST-minus-CONTROL traces, some of which are shown in Fig. 2. Curves 1 and 2 were obtained by fitting Eq. 1, with gap correction, to the two data sets. Curves 3, 4, and 5 were obtained by fitting a single Boltzmann distribution function, with CONTROL charge correction and gap correction, to the three data sets. The best fit parameters are:

Curve	c_m	$q_{\beta,max}/c_m$	$\overline{V}_\beta$	k_β	$q_{\gamma,max}/c_m$	$\overline{V}_\gamma$	k_γ
	μF/cm	*nC/μF*	*mV*	*mV*	*nC/μF*	*mV*	*mV*
1	0.143	10.0	−36.9	12.2	13.0	−62.0	1.7
2	0.148	4.5	−39.0	7.9	8.8	−55.9	2.6
3	0.158	6.7	−46.4	6.5			
4	0.175	3.6	−44.5	18.5			
5	0.195	0.9	−54.0	11.0			

in Fig. 6. Only data at TEST pulse potentials ≤ -30 mV were included in the analysis. The reason for this restriction is given in the Methods section of the preceding paper (Hui and Chen, 1992). Curves 1–3 were fitted to the three sets of data according to Eq. 4, with gap correction. Since the points at a V_H of −50 mV are essentially flat, consistent with the absence of Q_γ in curve 4 of Fig. 4, no curve was fitted to the points. The values of $q_{\gamma,max}/c_m$ listed in the legend of Fig. 6 show that Q_γ at a V_H of −70 mV was suppressed to 69.3% of control, very close to the value of 67.6% obtained with method 3 in Fig. 4. The agreement of the percentages of Q_γ remaining at a V_H of −70 mV obtained by methods 3 and 4 implies that the time

constant of I_γ during the post-pulse might not have changed when V_H was changed from −90 to −70 mV. Thus, there is a good chance that the time constant might be similar at a V_H of −60 mV.

Curve 3 of Fig. 6 reveals that Q_γ was not completely suppressed at a V_H of −60 mV

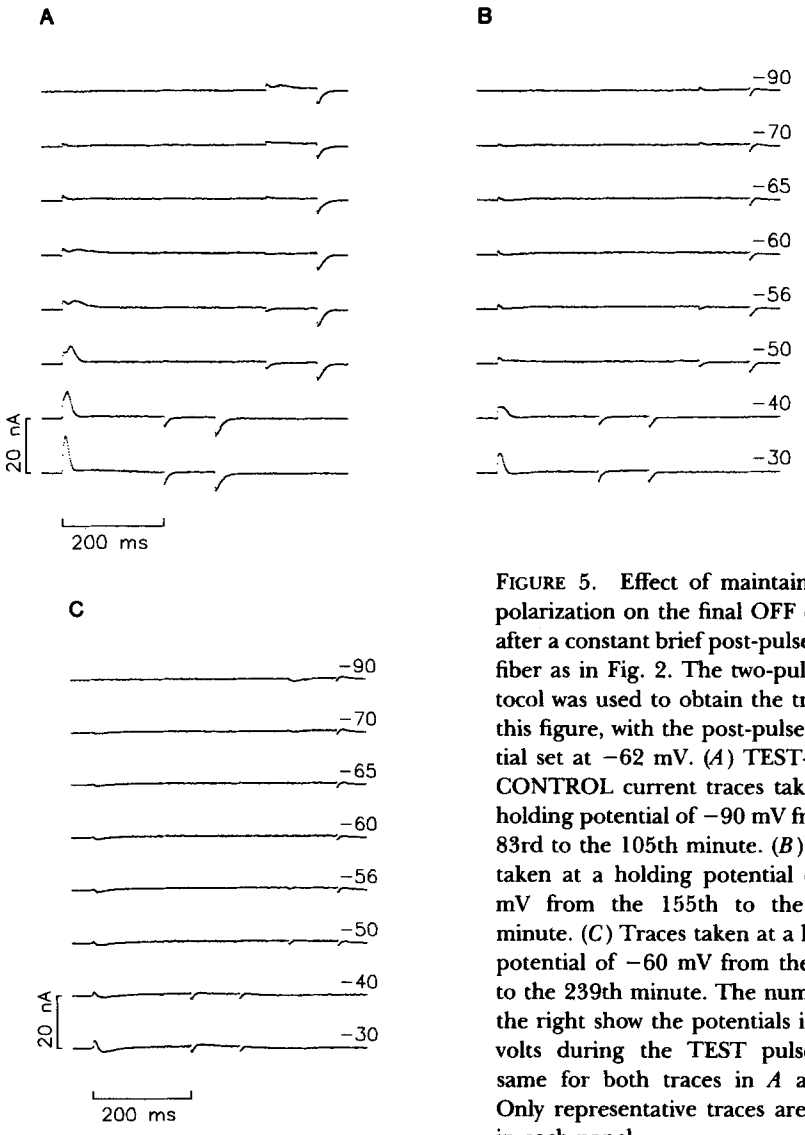

FIGURE 5. Effect of maintained depolarization on the final OFF current after a constant brief post-pulse. Same fiber as in Fig. 2. The two-pulse protocol was used to obtain the traces in this figure, with the post-pulse potential set at −62 mV. (*A*) TEST-minus-CONTROL current traces taken at a holding potential of −90 mV from the 83rd to the 105th minute. (*B*) Traces taken at a holding potential of −70 mV from the 155th to the 177th minute. (*C*) Traces taken at a holding potential of −60 mV from the 217th to the 239th minute. The numbers at the right show the potentials in millivolts during the TEST pulses (the same for both traces in *A* and *B*). Only representative traces are shown in each panel.

and the residual Q_γ was 5.3% of control. Thus, method 4 provides a more sensitive means to detect a small amount of Q_γ than method 3. Since the amount of Q_γ in curve 1 of Fig. 4 is 13.0 nC/μF, there ought to be 0.7 nC/μF of Q_γ in curve 3 of the same figure not resolvable by method 3. The amount of Q_β in curve 3 should

therefore be 6.0 nC/μF, equivalent to 60.1% for the residual Q_β at a V_H of −60 mV. The example given above illustrates the usefulness of method 4 in supplementing method 3 in separating charge components, at least qualitatively. Unfortunately, the residual amount of Q_β at a V_H of −60 mV so obtained still turned out to be larger than that at a V_H of −70 mV. This could be due to an underestimation of the value of $q_{\gamma,max}/c_m$ in curve 3 of Fig. 6 because of scatter of data.

The residual fractions of Q_β and Q_γ were studied in 26 cut fibers at different V_H's. Not all the levels of V_H were always used in each fiber. In experiments in which more than one V_H was used, the V_H was always changed monotonically in a depolarizing

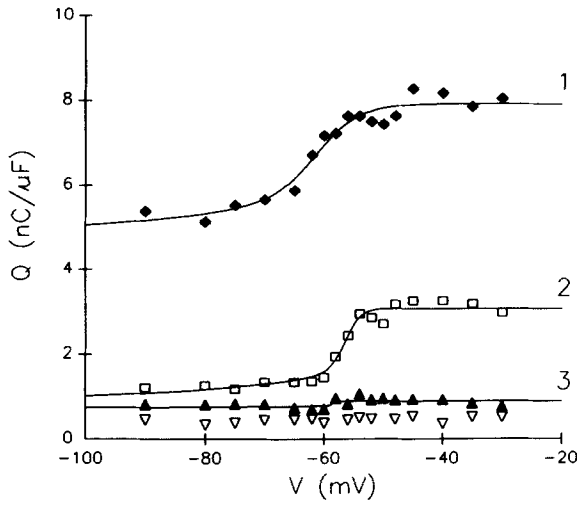

FIGURE 6. Effect of holding potential on steady-state voltage distribution of the final OFF charge after a constant brief post-pulse. Same fiber as in Fig. 2. ◆'s, □'s, ▲'s, and ▽'s show data taken at a holding potential of −90, −70, −60, and −50 mV, respectively. The points were obtained from time integrals of the final OFF transients (on repolarization from −62 to −90 mV) in TEST-minus-CONTROL current traces, some of which are shown in Fig. 5. Curves 1, 2, and 3 were obtained by fitting Eq. 4, with gap correction, to the three data sets. The best fit parameters are:

Curve	c_m	$q_{\gamma,max}/c_m$	$\overline{V}_\gamma$	k_γ
	μF/cm	*nC/μF*	*mV*	*mV*
1	0.142	3.0	−62.3	3.6
2	0.149	2.1	−57.0	1.3
3	0.160	0.2	−59.8	0.0

No curve was fitted to the ▽'s.

direction. The mean values for Q_β and Q_γ decreased monotonically when the level of V_H became less negative. On average, more Q_β was inactivated than Q_γ at a V_H of −70 mV, but more Q_γ was inactivated than Q_β at all V_H's ≥ −60 mV. The differences are all statistically significant ($P < 0.001$ for −70 and −30 mV, < 0.01 for −50 and −40 mV, and < 0.05 for −60 mV with the two-tailed t test).

The mean residual fractions of Q_β and Q_γ are plotted against V_H in Fig. 7. Curves 1 and 2 were fitted to the two sets of data according to Eq. 5. The best fit parameters are: for curve 1, $\overline{V}^*_\gamma = -64.8$ mV and $k^*_\gamma = 3.4$ mV; and for curve 2, $\overline{V}^*_\beta = -62.2$ mV and $k^*_\beta = 13.0$ mV. The values of k^*_γ and k^*_β for the inactivation curves in Fig. 7

are very close to the values of k_γ and k_β for the activation curves of Q_β and Q_γ, 2.9 and 11.0 mV given by Hui and Chandler (1990) or 2.7 and 10.7 mV given by Hui (1991*a*). Hence, the activation and inactivation curves of each charge component are mirror images of each other, the same as in intact fibers (Hui, 1983*b*).

From curve 2, the amount of mobile Q_β at a V_H of −90 mV is 0.89 of the asymptotic value. Strictly speaking, the amount should be exactly 1 by definition. In other words, the curve fitted to the open squares should be forced to pass through 1 at −90 mV. When this was done, the value of k_β was increased somewhat, which even exaggerated the general conclusion that the inactivation curve of Q_γ is steeper than that for Q_β. Considering the scatter of data, this refinement does not appear to be important.

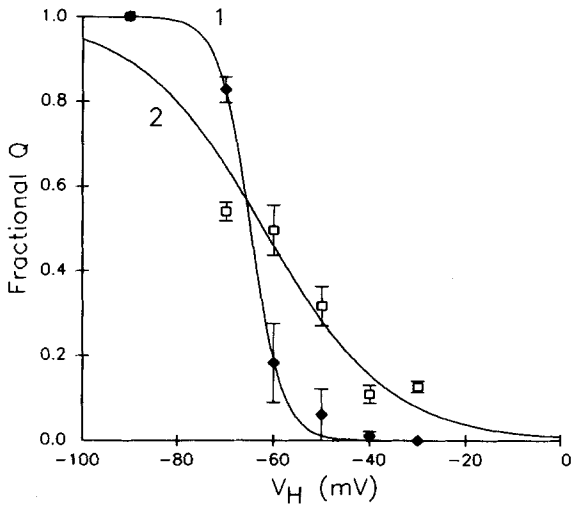

FIGURE 7. Steady-state inactivation curves of Q_β and Q_γ. □'s and ◆'s represent, respectively, the average fractions of Q_β and Q_γ that remain mobile at various holding potentials. The fractions at −90 mV are unity, by definition, for both charge components. The error bar for Q_γ at −30 mV is absent because the SEM is smaller than the size of the symbol. The two inverted sigmoidal curves 1 and 2 were fitted to the two data sets according to Eq. 5. n = 20, 5, 7, 5, and 3 at V_H = −70, −60, −50, −40, and −30 mV, respectively.

Reversibility of the Effect of Maintained Depolarization

In all the experiments reported here, a constant TEST pulse to −45 mV was always applied before, during, and after a sequence of runs that produced a *Q-V* plot to track the condition of the fiber at each V_H. In seven fibers the V_H was returned to −90 mV after a period of maintained depolarization to investigate whether the inactivation of Q_β and Q_γ was reversible. In one of the successful experiments, the control amount of OFF charge was 10.6 nC/μF. During a V_H of −70 and −60 mV, the average amounts of OFF charge were 8.1 and 5.3 nC/μF, respectively. On changing the V_H back to −90 mV, the average OFF charge was 8.7 nC/μF. In another fiber, the control amount of OFF charge was 14.0 nC/μF. During a V_H of −40 mV, the average amount of OFF charge was 0.9 nC/μF. On changing the V_H back to −90 mV, the average OFF charge was 11.0 nC/μF.

In the remaining five fibers, the amounts of OFF charge were less reversible even after a waiting period of 10–20 min upon repolarization. We believe that the

irreversibility observed was not likely to reflect a deterioration in the condition of the fibers, as judged from the relative stability of the linear cable parameters. There was an indication that part of the charge was still locked in the Q_α state, because the TEST-minus-CONTROL current traces after repolarization still showed some residual biphasic appearance similar to that in the traces of Fig. 2, *C* and *D*. The degree of persistence of the charge to stay in the inactivated state might depend on the magnitude and the duration of the maintained depolarization. Thus, for a finite period after repolarization, there might still be some uncertainty concerning the state of the fiber. Because of this complication, we are reluctant to chronically depolarize a fiber and apply CONTROL pulses in the positive potential range, as done by Brum and Rios (1987).

Inactivation Time Courses of Q_β and Q_γ

To study the inactivation time courses of Q_β and Q_γ, the family of TEST pulses that gave rise to one *Q-V* plot was individually preceded by the same conditioning depolarizing pulse having fixed magnitude and duration, and by a 240-ms resting period at −90 mV. Fig. 8 *A* shows TEST-minus-CONTROL current traces taken without conditioning depolarization. The traces in Fig. 8 *B* were taken with TEST pulses preceded by a 1-s conditioning pulse to −40 mV. Although the amplitudes of the I_β components and OFF transients in these traces are not very different from those in the corresponding traces of Fig. 8 *A*, the I_γ humps are much less pronounced. This crude visual analysis provides a hint that depolarization to −40 mV for just 1 s might inactivate more Q_γ than Q_β.

Fig. 8, *C* and *D*, shows traces taken with TEST pulses preceded by a conditioning pulse to −40 mV lasting 5 and 20 s, respectively. As the duration of the conditioning pulse was increased, both the ON and OFF transients in the traces were suppressed progressively. There is no sign of any I_γ hump in the ON segments of the traces in Fig. 8 *D*. The OFF transients in these traces decay faster than those in Fig. 8 *A*, probably because the OFF transients in Fig. 8 *D* consist purely of I_β, which decays faster than I_γ in cut fibers (Hui and Chandler, 1991). At the end of the experiment, the V_H was changed to −40 mV and traces similar to those of Fig. 2 *D* were taken (not shown). These traces provided information about the steady-state inactivation of Q_β and Q_γ at −40 mV.

The amounts of OFF charge in the traces of Fig. 8, and other traces not shown, are plotted against TEST pulse potential in Fig. 9. Curves 1, 2, and 3 were fitted to the data taken without and with 1 and 5 s conditioning depolarization, respectively, according to Eq. 1, with gap correction. The values of $q_{i,max}/c_m$ listed in the figure legend show that 1 s conditioning depolarization to −40 mV changed the amounts of Q_β and Q_γ to 108.1 and 73.1% of control values, and 5 s conditioning depolarization to 86.6 and 32.7%, respectively. The data taken with 20 s conditioning depolarization could not be fitted by Eq. 1 but were fitted well by a single Boltzmann distribution function with CONTROL charge correction and gap correction, represented by curve 4. Since the I_γ hump is absent in the traces of Fig. 8 *D*, the residual charge in curve 4 is assumed to belong to Q_β and is 53.8% of control.

The percentages of Q_β and Q_γ that remained mobile are plotted against the duration of the conditioning depolarization in Fig. 10. The two smooth curves show

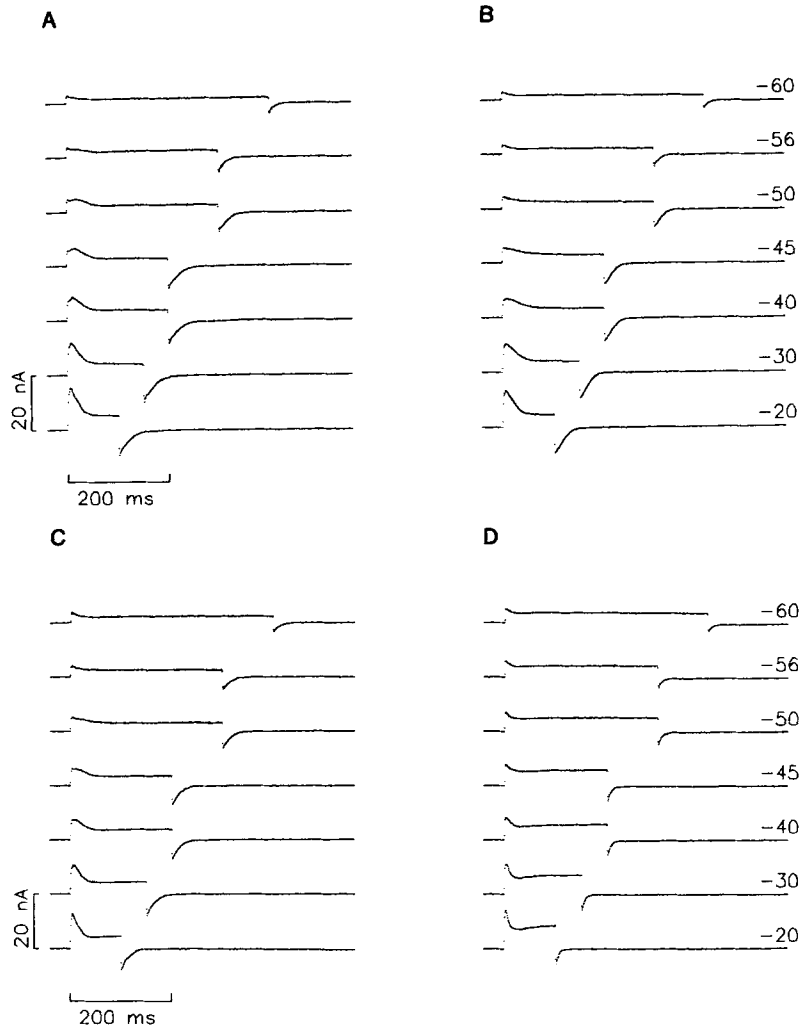

FIGURE 8. Effect of the duration of conditioning depolarization on TEST-minus-CONTROL current in a cut fiber. Fiber identification: 97171. Diameter = 99 μm. Sarcomere length = 3.5 μm. Saponin treatment was applied to membrane segments in both end pools at time zero. After rinsing, the solutions in the end pools were replaced by solution B. The solution in the center pool was then changed to an isotonic TEA·Cl solution (solution D). At the 22nd minute the voltage clamp was turned on and the holding potential was set at −90 mV. From the beginning to the end of the experiment the holding current changed from −24 to −30 nA and $r_e/(r_e + r_i)$ decreased from 0.987 to 0.985. The fiber was stimulated by the one-pulse protocol. (*A*) Traces recorded from the 59th to the 79th minute with TEST pulses alone. (*B*) Traces recorded from the 99th to the 136th minute with TEST pulses, each of which was preceded by a conditioning prepulse to −40 mV for 1 s. (*C*) Traces recorded from the 178th to the 211st minute with TEST pulses, each preceded by a conditioning prepulse to −40 mV for 5 s. (*D*) Traces recorded from the 167th to the 216th minute with TEST pulses, each preceded by a conditioning prepulse to −40 mV for 20 s. The numbers at the right show the potentials in millivolts during the TEST pulses (the same for both traces in the same row). Only representative traces are shown in each panel.

the decay time courses of Q_β and Q_γ. Curve 2 was obtained by fitting a single exponential, whereas curve 1 was obtained by fitting a single exponential plus 1.3 nC/μF, which is the value of $q_{\beta,max}/c_m$ obtained from the Q-V plot at a V_H of −40 mV. The time constants for the inactivation of Q_β and Q_γ at −40 mV are 25 and 3.4 s, respectively, in this fiber, confirming the above observation that Q_γ is inactivated faster than Q_β.

Similar experiments were performed on four other fibers and the inactivation time constant of Q_β is longer than that of Q_γ in all fibers. In one of the four fibers, the inactivation time constants of Q_β and Q_γ are 59 and 5.3 s at −40 mV. Averaging

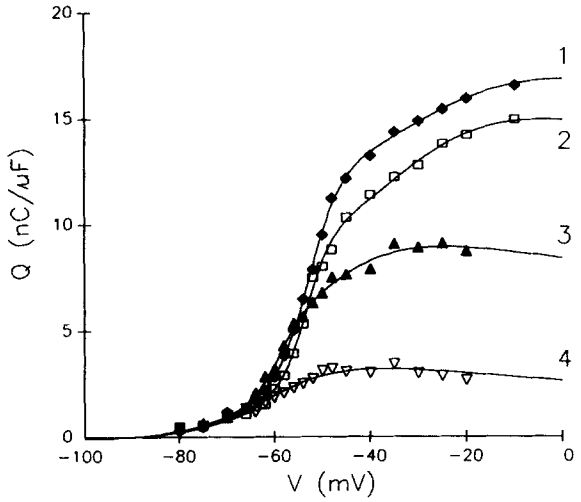

FIGURE 9. Effects of the duration of conditioning prepulse on steady-state voltage distributions of Q_β and Q_γ. Same fiber as in Fig. 8. ◆'s show data taken with TEST pulses alone, and □'s, ▲'s, and ▽'s with TEST pulses preceded by a conditioning prepulse to −40 mV for 1, 5, and 20 s, respectively. The points were obtained from time integrals of OFF current transients in TEST-minus-CONTROL traces, some of which are shown in Fig. 8. Curves 1, 2, and 3 were obtained by fitting Eq. 1, with gap correction, to the three data sets. Curve 4 was obtained by fitting a single Boltzmann distribution function, with CONTROL charge correction and gap correction, to the other data set. The best fit parameters are:

Curve	$q_{\beta,max}/c_m$	$\overline{V}_\beta$	k_β	$q_{\gamma,max}/c_m$	$\overline{V}_\gamma$	k_γ
	nC/μF	*mV*	*mV*	*nC/μF*	*mV*	*mV*
1	9.0	−32.4	12.8	12.6	−53.8	3.3
2	9.1	−35.1	10.1	9.2	−54.4	2.6
3	7.8	−51.8	8.6	4.1	−60.2	2.6
4	4.8	−62.9	7.6			

between the two fibers, the inactivation time constants of Q_β and Q_γ at −40 mV are 42 and 4.4 s. From two of the other fibers, the average values for the inactivation time constants of Q_β and Q_γ at −30 mV are 29 and 5.0 s. The inactivation time constants of Q_β and Q_γ at −50 mV were studied in only one fiber and the values are 45 and 9.7 s. These values vaguely suggest a voltage-dependent decrease in inactivation time constant for either Q_β or Q_γ when V_H becomes less negative. However, more experiments will be required to establish the detailed voltage dependencies of the inactivation time constants.

Effect of Multiple Stimulation on Q_γ in the Presence of 20 mM Internal EGTA

The last group of experiments was performed to investigate whether the I_γ hump indeed disappears during repetitive stimulation. Several experiments were first carried out with 20 mM EGTA in the internal solution, the same as in most of our cut fiber experiments. In these experiments each CONTROL run was accompanied by two TEST runs separated by 6 s. The same CONTROL current trace was scaled and subtracted from the first and second TEST current traces to generate the TEST-minus-CONTROL current traces shown in the same row of Fig. 11, *A* and *B*, respectively. The I_γ humps present in the first TEST runs at −50 and −45 mV disappear in the second TEST runs, whereas those at −40 and −35 mV are suppressed in the second TEST runs. Those at −30 and −20 mV appear to be affected very little.

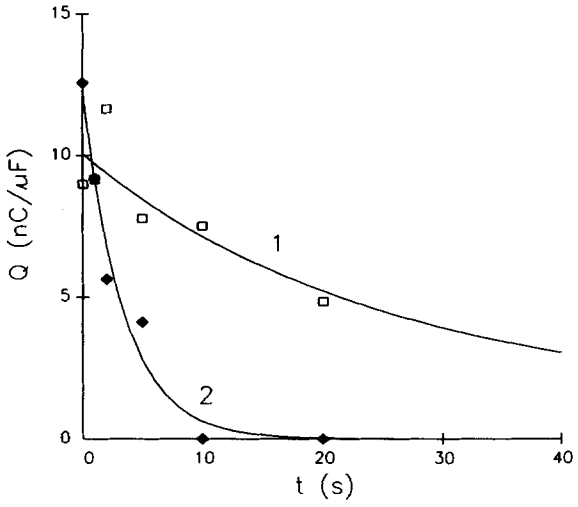

FIGURE 10. Inactivation time course of Q_β and Q_γ at −40 mV. Same fiber as in Fig. 8. The value of $q_{i,max}/c_m$ (i = β or γ) is plotted as a function of duration of the conditioning prepulse to −40 mV. □'s and ◆'s represent, respectively, values of $q_{\beta,max}/c_m$ and $q_{\gamma,max}/c_m$ obtained from *Q-V* plots, some of which are shown in Fig. 9. Each set of data is fitted by a single exponential decay function. The curve for Q_β is constrained to approach an asymptotic value of 1.3 nC/μF, which is the value of $q_{\beta,max}/c_m$ at a holding potential of −40 mV. The decay time constants for Q_β and Q_γ are 25 and 3.4 s, respectively.

To examine the change in shape of the I_γ humps more closely, each trace in Fig. 11 *B* was subtracted from the corresponding trace in Fig. 11 *A*. The difference traces are shown in Fig. 11 *C*. The amplitude of the OFF transient increases from the first difference trace to the second and then decreases in the lower difference traces. More surprisingly, except for the first one, every difference trace seems to have more ON charge than OFF charge. These peculiarities can be explained by the analyses shown in the next two figures.

The third trace in Fig. 11 *C* appears to have the largest inequality between ON and OFF charge and is selected to illustrate the point. The trace is shown in expanded scale as the lower trace in Fig. 12. Line 1 was obtained by least-squares fitting a sloping straight line to the last 200 ms in the ON segment and corresponded to a

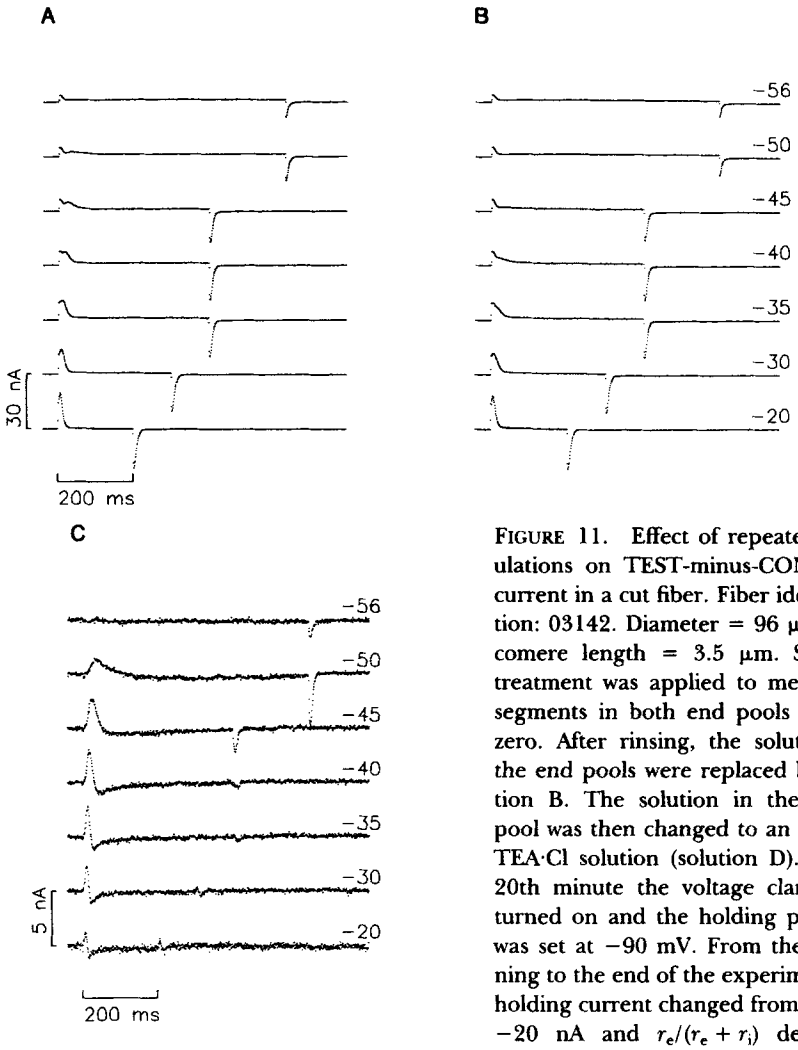

FIGURE 11. Effect of repeated stimulations on TEST-minus-CONTROL current in a cut fiber. Fiber identification: 03142. Diameter = 96 μm. Sarcomere length = 3.5 μm. Saponin treatment was applied to membrane segments in both end pools at time zero. After rinsing, the solutions in the end pools were replaced by solution B. The solution in the center pool was then changed to an isotonic TEA·Cl solution (solution D). At the 20th minute the voltage clamp was turned on and the holding potential was set at −90 mV. From the beginning to the end of the experiment the holding current changed from −14 to −20 nA and $r_e/(r_e + r_i)$ decreased from 0.993 to 0.991. For each TEST potential shown at the right in millivolts, a CONTROL current trace was taken first and then two TEST current traces were elicited by identical TEST pulses applied 6 s apart. The fiber was allowed to rest for 5 min before another group of CONTROL and TEST current traces at another potential was taken. The TEST-minus-CONTROL current traces obtained by subtracting the CONTROL current trace from the first and second TEST current traces are shown in *A* and *B*, respectively. The difference of two traces in the same row of *A* and *B* is shown in the corresponding row of *C*. The amounts of OFF charge in the difference traces are (from top to bottom): 1.8, 4.9, 2.7, 1.0, 0.3, −0.1, and 1.7 nC/μF. A negative value implies that the amount of OFF charge in the second TEST run is larger than that in the first TEST run at the same potential. Traces were taken from the 55th to the 165th minute. Only representative traces are shown in each panel.

baseline one would pick visually. With line 1 as baseline, the ON charge is 9.8 nC/μF, which is much larger than the 2.7 nC/μF of OFF charge listed in the legend of Fig. 11. On the other hand, if the ionic current did not change from the first TEST run to the second TEST run, then the time axis, represented by the thin line numbered 2, should be the baseline for the ON segment. With this baseline, the ON charge is −4.9 nC/μF, indicating that the assumption that the ionic current did not change was incorrect.

Unfortunately, there is no objective approach to determine exactly by how much the ionic current had changed in the second TEST run. However, if line 2 is artificially shifted downward by 0.19 nA, the new baseline represented by line 3 gives an ON charge that matches the OFF charge exactly. A small shift of 0.19 nA in the maintained current is quite probable and line 3 actually fits the points at the end of

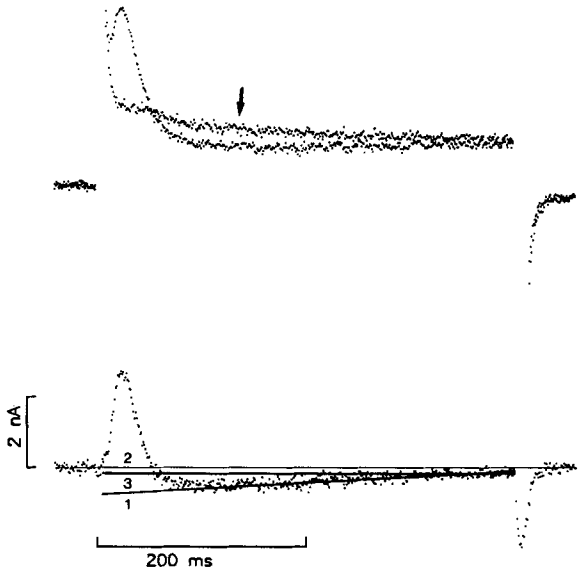

FIGURE 12. Change in time course of the I_γ hump during repetitive stimulation. Same fiber as in Fig. 11. The upper pair of traces is replotted from the third traces in Fig. 11, *A* and *B*, and superimposed on each other. The first 9 points in the ON transients and the first 15 points in the OFF transients are off scale. The lower trace is replotted from the third trace in Fig. 11 *C*. Line 1 was fitted by least squares to the last 200 ms of the ON segment. Line 2 is the time axis corresponding to zero current. Line 3 was obtained by shifting line 2 downward by 0.19 nA such that the net ON charge matches the OFF charge.

the interval very well. If line 3 is indeed the baseline for the ON segment, then the difference current in this segment is biphasic. This could explain the presence of a negative phase in difference charge movement traces observed by Csernoch et al. (1989). This appearance has been observed on other occasions (Hui, 1991*b*; Hui and Chen, 1992). A likely explanation for the appearance is that the I_γ hump became very broad in the second TEST run and that the slow positive tail of the I_γ component (marked by the arrow in Fig. 12*A*) gave rise to the slow negative phase in the difference trace. This example shows that, in this fiber, even a pulse of 400 ms duration to −45 mV was not sufficiently long to permit a reliable fit of the ON baseline. One should therefore be particularly cautious in drawing information from ON segments of difference traces at potentials just above the activation threshold of Q_γ.

The amounts of OFF charge in the traces of Fig. 11, *A* and *B*, and others not shown, are plotted against TEST pulse potential in Fig. 13. Filled diamonds and open squares represent, respectively, the amounts of charge in the first and second TEST runs. From here on, the *Q-V* plot based on the *i*th TEST runs will be called the *i*th *Q-V* plot. The two *Q-V* plots in Fig. 13 appear to have similar shapes and magnitudes, but the second *Q-V* plot is displaced by a few millivolts to the right along the voltage axis, similar to the effect of 25 μM tetracaine (Fig. 3 in Hui and Chen, 1992). Curves 1 and 2 were fitted to the two data sets, according to Eq. 1, with gap correction. The best fit parameters listed in the figure legend show that $\overline{V}_\gamma$ in curve 2

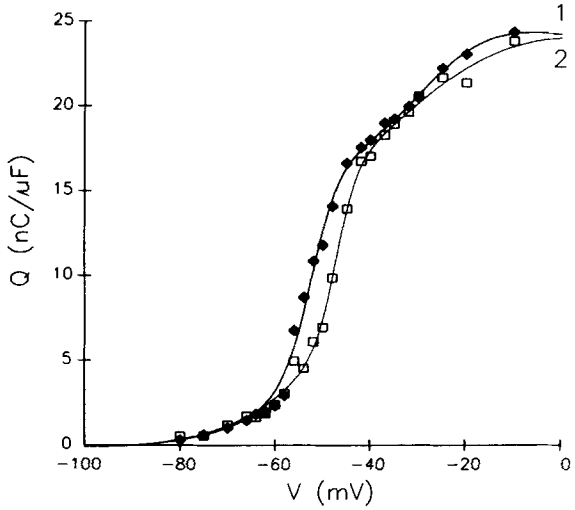

FIGURE 13. Effects of repeated stimulations on steady-state voltage distributions of Q_β and Q_γ. Same fiber as in Fig. 11. ◆'s and □'s were obtained from time integrals of OFF current transients in TEST-minus-CONTROL traces in Fig. 11, *A* and *B*, respectively, and other traces not shown. Curves 1 and 2 were obtained by fitting Eq. 1, with gap correction, to the two data sets. The best fit parameters are:

Curve	$q_{\beta,max}/c_m$	$\overline{V}_\beta$	k_β	$q_{\beta,max}/c_m$	$\overline{V}_\gamma$	k_γ
	nC/μF	*mV*	*mV*	*nC/μF*	*mV*	*mV*
1	10.8	−29.0	7.3	17.9	−53.1	3.0
2	15.6	−33.7	12.8	13.6	−47.8	2.2

is 5.3 mV less negative than that in curve 1, consistent with the shift observed visually. $q_{\gamma,max}/c_m$ turns out to be 4.3 nC/μF smaller in curve 2 than in curve 1, but $q_{\beta,max}/c_m$ is 4.8 nC/μF larger. This could be a real effect of double stimulation. Alternatively, part of the change could be due to scatter of data, as explained in the Discussion of the preceding paper (Hui and Chen, 1992). If the latter is true, the mere effect of double stimulation is a shift of the *Q-V* plot slightly to the right. The shift in the *Q-V* plot explains why the OFF charge is largest at −50 mV in the difference traces of Fig. 11 *C*; it is because that particular potential falls on the steepest part of the *Q-V* curve.

Experiments of the same kind were performed on three other fibers. The average changes in the six Boltzmann parameters from the first *Q-V* plot to the second are listed in the first row of Table II. The only statistically significant change was the increase in $\overline{V}_\gamma$. Thus, the changes in $q_{\beta,max}/c_m$ and $q_{\gamma,max}/c_m$ observed in Fig. 13 were probably due to scatter of data.

Effect of Increasing [EGTA]$_i$ from 20 to 50 mM on Charge Movement

If Q_γ is a consequence of Ca release, the 20 mM EGTA in the internal solution might not be high enough to effectively deplete the SR of releasable Ca or to effectively prohibit the Ca^{2+} released from the SR to reach the tubular membrane, thereby resulting in very little change in Q_γ during repetitive stimulation. To definitively rule out this possibility, additional experiments were carried out with all the glutamate in

TABLE I

Comparison of Q-V Distributions of Q_β and Q_γ with 20 and 50 mM EGTA in the End-Pool Solution

	(1) $\overline{V}_\beta$	(2) k_β	(3) $q_{\beta,max}/c_m$	(4) $\overline{V}_\gamma$	(5) k_γ	(6) $q_{\gamma,max}/c_m$
	mV	*mV*	*nC/μF*	*mV*	*mV*	*nC/μF*
20 mM EGTA						
Mean	−41.7	11.2	10.5	−58.9	2.6	13.1
SEM	3.4	1.9	1.0	1.9	0.3	1.0
50 mM EGTA						
Mean	−38.5	9.9	12.4	−61.8	3.5	12.4
SEM	3.2	0.9	1.4	1.2	0.3	1.3
P	>0.5	>0.5	>0.2	>0.2	<0.05	>0.5

Results were collected from eight fibers. Columns 1–6 give the mean values and the SEMs of the best fit parameters obtained by fitting *Q-V* plots with a sum of two Boltzmann distribution functions, with CONTROL charge correction and gap correction. The last row gives the significance of the differences between the two sets of values, with the two-tailed *t* test.

the internal solution replaced isosmotically by EGTA (solution C) and the $[EGTA]_i$ increased to 50 mM. Before the study of repetitive stimulation with this internal solution, experiments were carried out to check whether the increase in $[EGTA]_i$ had any direct effect on charge movement. Results from eight experiments are summarized in Table I. The results show that increasing $[EGTA]_i$ from 20 to 50 mM has minimal effect on the amounts or voltage distributions of Q_β or Q_γ. 50 mM EGTA did appear to increase the value of k_γ somewhat and make the I_γ hump less prominent, probably due to a broadening of the waveform of the hump.

Effect of Multiple Stimulation on Q_γ in the Presence of 50 mM Internal EGTA

If Q_γ is a consequence of Ca release, a train of only two stimulations (Fig. 11) might not be sufficient to effectively deplete the SR of releasable Ca. In the following group

of experiments carried out with 50 mM internal EGTA, the number of stimulations at each TEST potential was increased to 3, 5, or 10. Results from one of the experiments are shown in Figs. 14–16.

In this experiment, a train of 10 TEST pulses was applied at each potential at a frequency of one per 6 s. Again, the same CONTROL current trace was used to subtract the linear currents from all 10 TEST current traces. Since 15 min of recovery time was allowed between each train of stimulations, charge movement was studied at fewer TEST potentials than with the usual one- or two-pulse protocol. Fig. 14 *A* shows TEST-minus-CONTROL current traces obtained from the first TEST runs. The traces resemble those recorded from fibers with 20 mM EGTA in the internal solution. The traces obtained from the second TEST runs (Fig. 14 *B*) still show very prominent I_γ humps. The changes in the shapes of the I_γ humps can be visualized more easily by taking pairwise differences of the traces in Fig. 14, *A* and *B*, as shown in Fig. 15 *A*. The amount of OFF charge in all the difference traces was <1 nC/μF (see Fig. 15 legend). The biphasic ON transients can be explained by a broadening of the I_γ waveform (see text associated with Fig. 12).

The traces in Fig. 14 *C* were obtained from the third TEST runs. They look exactly the same as the traces from the second TEST runs. In fact, the difference traces between the second and third TEST runs (Fig. 15 *B*) are essentially flat. The traces obtained from all subsequent TEST runs are all identical to the corresponding traces from the third TEST run. Only the traces obtained from the tenth TEST runs are shown in Fig. 14 *D*. The difference traces obtained by subtracting the traces in Fig. 14 *D* from the corresponding traces in Fig. 14 *C* are also flat (not shown). The persistence of the I_γ humps even in the tenth stimulation is in contrast to the finding of Garcia et al. (1990), who observed a disappearance of the hump during repetitive stimulation. The 62.5 mM EGTA they used was slightly higher than the 50 mM used in this experiment. However, the fiber in this experiment was stimulated at a much higher frequency.

The amounts of OFF charge in the traces from the first, second, and tenth TEST runs (Fig. 14, *A*, *B*, and *D*, and others not shown) are plotted against TEST pulse potential in Fig. 16. Those from the third TEST runs (Fig. 14 *C*) are not shown to avoid overlap. The three *Q-V* plots are not very different from each other. Curves 1–3 were fitted to the three data sets, according to Eq. 1, with gap correction. The best fit parameters are listed in the figure legend. Compared with the values in curve 1, $q_{\beta,max}/c_m$ in curve 2 is decreased to 85.9%, $\overline{V}_\beta$ is shifted by −0.6 mV, k_β is decreased by 1.1 mV, $q_{\gamma,max}/c_m$ is increased to 103.9%, $\overline{V}_\gamma$ is shifted by +1.1 mV, and k_γ is increased by 0.7 mV. Also, $q_{\beta,max}/c_m$ in curve 3 is decreased to 76.9%, $\overline{V}_\beta$ is shifted by +1.1 mV, k_β is decreased by 1.7 mV, $q_{\gamma,max}/c_m$ is increased to 101.0%, $\overline{V}_\gamma$ is shifted by +2.1 mV, and k_γ is decreased by 0.2 mV.

Similar experiments were performed on six other fibers. In two of the experiments, trains of 10 TEST pulses were applied at each potential as in the experiment just shown, whereas in the other four experiments only trains of three or five TEST pulses were applied. The average changes in the Boltzmann parameters for the second, third, and tenth *Q-V* plots are listed in the second, third, and fourth rows of Table II. All the changes are statistically insignificant with the two-tailed *t* test, except for the

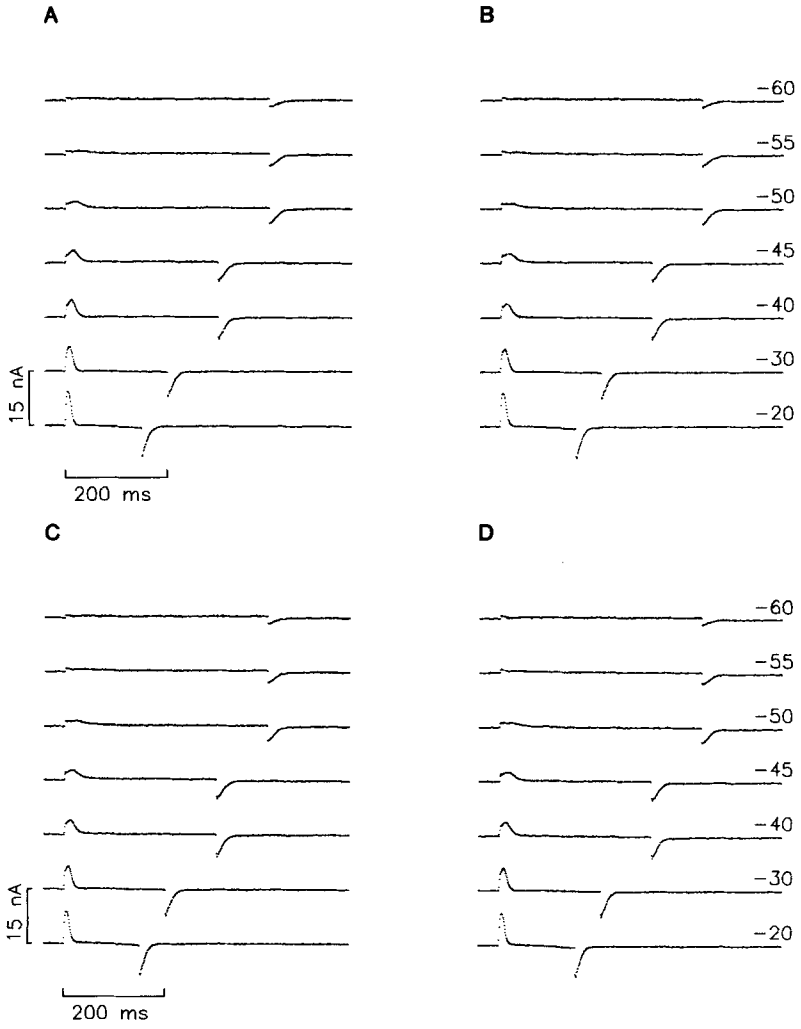

FIGURE 14. Effect of multiple stimulations on TEST-minus-CONTROL current in a cut fiber with 50 mM EGTA in the internal solution. Fiber identification: 04261. Diameter = 87 μm. Sarcomere length = 3.5 μm. Saponin treatment was applied to membrane segments in both end pools at time zero. After rinsing, the solutions in the end pools were replaced by solution C containing 50 mM EGTA. Then the solution in the center pool was changed to an isotonic TEA·Cl solution (solution D). At the 22nd minute the voltage clamp was turned on and the holding potential was set at −90 mV. From the beginning to the end of the experiment the holding current changed from −14 to −18 nA and $r_e/(r_e + r_i)$ remained constant at 0.992. For each TEST potential shown at the right in millivolts, a CONTROL current trace was taken first and then 10 TEST current traces were elicited by a train of identical TEST pulses at a rate of one per 6 s. The fiber was allowed to rest for 15 min before another group of CONTROL and TEST current traces at another potential was taken. The TEST-minus-CONTROL current traces obtained by subtracting the CONTROL current trace from the 1st, 2nd, 3rd, and 10th TEST current traces are shown in *A*, *B*, *C*, and *D*, respectively, in the same row. Traces were taken from the 60th to the 256th minute. Only representative traces are shown in each panel.

decrease in $q_{\beta,max}/c_m$ in the second Q-V plots and the shift in $\overline{V}_\gamma$ in the third Q-V plots, but even these two changes are marginally significant.

Although a train of ≤ 10 stimulations had a negligible effect on Q_γ, one could argue that the stimulation rate of once per 6 s could be too slow to bring about a noticeable effect. Four experiments were done to test this idea by making use of the double-pulse protocol, in which each pair of TEST pulses was applied with a 400-ms time gap in between. Interestingly, the I_γ hump in the ON segment of the second pulse was still almost as prominent as that of the first. Moreover, a steeply rising component still existed in the second Q-V plot and was similar to that in the first Q-V plot.

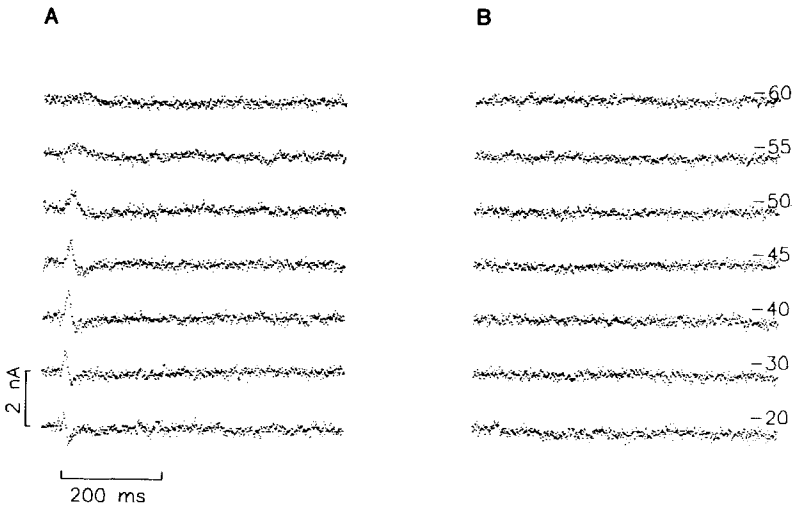

FIGURE 15. Difference current traces between two successive stimulations from a cut fiber with 50 mM EGTA in the internal solution. Same fiber as in Fig. 14. Each trace was obtained from the difference of the two corresponding traces in Fig. 14, *A* and *B* (*A*) or in Fig. 14, *B* and *C* (*B*). The amounts of OFF charge in the difference traces in *A* are (from top to bottom): 0.3, 0.6, 0.4, 0.0, 0.0, 0.1, and −0.1 nC/μF. A negative value implies that the amount of OFF charge in the second TEST run is larger than that in the first TEST run at the same potential. The amounts of OFF charge in the difference traces in *B* are all negligible.

DISCUSSION

Steady-State Inactivation of Q_β and Q_γ by Maintained Depolarization

Steady-state inactivation of charge movement was studied in intact fibers by several investigators (Adrian and Almers, 1976; Rakowski, 1981; Hui, 1983*b*; Rakowski et al., 1985). In most of the studies (except Hui, 1983*b*) the amounts of charge were not separated into Q_β and Q_γ components and so only inactivation curves of the total charge were obtained. It was found that the inactivation curve of the total charge was roughly a mirror image of the activation curve.

In this paper the inactivation of charge movement was studied in cut fibers and the differential inactivation properties of Q_β and Q_γ were separated. Fig. 7 shows that the inactivation of Q_β is less voltage dependent than that of Q_γ, in good agreement with the results obtained from intact fibers (Hui, 1983*b*). The curves in the figure were fitted by assuming that the voltage dependence of inactivation of each charge component follows an inverse sigmoidal function. Under this assumption, the k factors for the activation and inactivation curves of Q_β are roughly the same, ~11–13 mV, and likewise for the curves of Q_γ, ~3 mV. This implies that, for each charge species, the activation and inactivation curves are mirror images of each other.

A consequence of the shallow inactivation curve of Q_β is that it crosses the

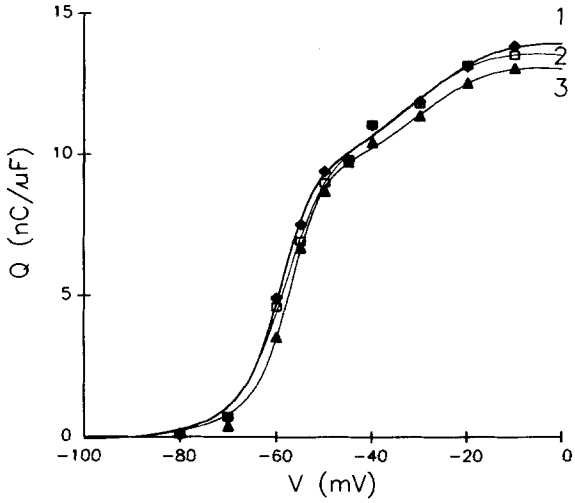

FIGURE 16. Effects of multiple stimulations on steady-state voltage distributions of Q_β and Q_γ from a cut fiber with 50 mM EGTA in the internal solution. Same fiber as in Fig. 14. ◆'s, □'s, and ▲'s were obtained from time integrals of OFF current transients in TEST-minus-CONTROL traces in Fig. 14, *A*, *B*, and *D*, respectively, and other traces not shown. Curves 1, 2, and 3 were obtained by fitting Eq. 1, with gap correction, to the three data sets. The best fit parameters are:

Curve	*Q-V* plot	$q_{\beta,max}/c_m$	$\overline{V}_\beta$	k_β	$q_{\gamma,max}/c_m$	$\overline{V}_\gamma$	k_γ
		nC/μF	*mV*	*mV*	*nC/μF*	*mV*	*mV*
1	1st	7.8	−30.9	10.6	10.4	−59.7	3.4
2	2nd	6.7	−31.5	9.5	10.8	−58.6	4.1
3	10th	6.0	−29.8	8.9	10.5	−57.6	3.2

inactivation curve of Q_γ at a potential > -70 mV. Thus, at -70 mV a larger proportion of Q_β is inactivated than Q_γ. This implies that it is unlikely to have *all* Q_β serve as voltage sensors for triggering Ca release and all Q_γ arise as a result of the release, because it is difficult to imagine how a larger reduction in the amount of moveable sensors can lead to a smaller reduction in the quantity of end products. The shallow inactivation curve of Q_β can be explained by a possible multi-component nature of Q_β (see Discussion sections in Chen and Hui, 1991*a*; Hui, 1991*b*). Each component might have a different inactivation curve and some of the curves can be more steeply voltage dependent than the others. A summation of all the curves with a spread in the values of $\overline{V}^*$ and k^* can yield a shallow resultant inactivation curve.

Another consequence of the shallow inactivation curve of Q_β is that the amount of moveable Q_β does not reach full value at a V_H of −90 mV. The curve predicts that when V_H is made more negative $q_{\beta,max}/c_m$ should increase, which has indeed been observed by Hui (1991*b*).

Adrian and Peres (1979) separated Q_β and Q_γ by assuming that at −40 mV Q_γ is completely inactivated, whereas Q_β is fully mobile. Fig. 7 shows that Q_γ is completely inactivated at −40 mV in our cut fibers, but only a small fraction of Q_β remains mobile. At more negative levels of V_H, more Q_β remains mobile but then Q_γ is not completely inactivated. There is no V_H at which the separation method of Adrian and Peres (1979) can yield Q_β and Q_γ components that are equivalent to those separated by any of the four methods used in the preceding paper (Hui and Chen, 1992).

TABLE II

Change in Boltzmann Parameters in the ith Q-V Plot Compared with Those in the First Q-V Plot

(1)	*(2)*	*(3)*	*(4)*	*(5)*	*(6)*	*(7)*	*(8)*	*(9)*	*(10)*
i	[EGTA]	Δt	$\Delta\overline{V}_\beta$	Δk_β	$q_{\beta,max}/c_m$ ratio	$\Delta\overline{V}_\gamma$	Δk_γ	$q_{\gamma,max}/c_m$ ratio	n
	mM	*s*	*mV*	*mV*	%	*mV*	*mV*	%	
2	20	6	3.8	3.8	108	4.1	0.9	104	4
			(>0.3)	(>0.2)	(>0.5)	(<0.02)	(>0.3)	(>0.8)	
2	50	6	5.3	0.8	79	3.5	1.2	118	7
			(>0.1)	(>0.5)	(<0.05)	(>0.05)	(>0.05)	(>0.5)	
3	50	6	6.1	1.5	90	4.3	1.2	114	7
			(>0.1)	(>0.3)	(>0.3)	(<0.05)	(>0.05)	(>0.5)	
10	50	6	2.7	−0.9	85	4.7	0.8	102	3
			(>0.3)	(>0.5)	(>0.4)	(>0.3)	(>0.2)	(>0.8)	

Two groups of experiments were performed. In the first group listed in the first row, pairs of two identical TEST pulses were applied at different potentials at a rate of one pair per 5 min. The second group listed in the second to fourth rows was performed on seven fibers. In three of the fibers, trains of 10 TEST pulses were applied at a rate of one train per 10 or 15 min. In the remaining four fibers, trains of three or five identical TEST pulses were applied at the same rate. Columns 1 and 2 give the values of i for the ith Q-V plot (see definition in text) and the concentrations of EGTA. Column 3 gives the time separation between successive TEST pulses in a pair or a train. Columns 4–9 give the average changes in the values of the Boltzmann parameters from the first Q-V plot to the ith Q-V plot. $\Delta\overline{V}_i$ or Δk_i were calculated by subtracting the value in the first Q-V plot from the corresponding value in the ith Q-V plot. $q_{i,max}/c_m$ ratio was calculated by dividing the value in the ith Q-V plot by the corresponding value in the first Q-V plot. The statistical significance of each change, estimated with the two-tailed t test, is shown in parenthesis below each value. Column 10 gives the number of fibers included in the average.

Inactivation Time Courses of Q_β and Q_γ

Chandler et al. (1976) found that the total charge was inactivated with a time constant of 10–25 s at −20 mV and 1°C. Adrian and Almers (1976) found that the half-time for inactivation of the total charge was ~2 min at −50 mV and 2–6°C. Rakowski (1981) suggested a voltage dependence of the inactivation time constant for the total charge. These results were obtained from intact fibers. If the charge movement they measured contained Q_γ, the time constants they obtained should be lumped values for both Q_β and Q_γ. In this work, Q_β and Q_γ were separated in cut fibers by method 3 and were found to follow different time courses in inactivation. At

−50 to −30 mV the inactivation time constant of Q_β is 5–10-fold as large as that of Q_γ. There is also a suggestion of both time constants becoming smaller at a less negative potential.

Comparison with Inactivation of Tension Generation or Ca Indicator Signal

To gain insight into the possible physiological role(s) of Q_β and Q_γ in excitation–contraction coupling, it is of interest to compare the voltage dependencies of inactivation of Q_β and Q_γ with those of tension and rise in $[Ca^{2+}]_i$. Inactivation of K contracture tension was found to be steeply voltage dependent and the inactivation curve was almost a mirror image of the activation curve (Hodgkin and Horowicz, 1960; Luttgau and Glitsch, 1976). Although the k factor of the inactivation curve was not determined, contracture tension inactivated almost fully over a 20-mV range of potential, which correlates much better with the inactivation curve of Q_γ in Fig. 7 than that of Q_β.

To the best of our knowledge, the effect of changing V_H on Ca release has only been studied by Rakowski et al. (1985). They monitored the rise in $[Ca^{2+}]_i$ with the indicator arsenazo III and found that the peak rate of absorbance change also inactivated steeply over a range of V_H of ~20 mV. The curve was steeper than the inactivation curve or the activation curve of the total charge obtained from the same fiber. Hence, the inactivation curve of Q_γ in Fig. 7 correlates well with the inactivation curve of the absorbance signal.

The time course of inactivation of Ca release has not yet been studied. This should be an important experiment providing useful information to support the role(s) of Q_β and Q_γ.

Effect of Repetitive Stimulation on I_γ Hump

The results presented in this paper do not agree with the conclusion drawn by Garcia et al. (1990). With the experimental protocol used in this work, pronounced I_γ humps could still be observed in TEST-minus-CONTROL current traces, and a substantial Q_γ component could still be resolved in Q-V plots after repetitive stimulation. The I_γ hump they recorded at −20 mV resembles the hump we obtained at ~−45 mV (Fig. 11 *A*). These potentials fall on the steeply rising parts of the respective Q-V plots. The disappearance of the I_γ hump they observed could be caused merely by a shift of the Q_γ-V plot to the right. Fig. 12 also shows that the difference current trace between the first and second TEST runs at such a potential might erroneously yield an apparent inequality between ON and OFF charge if the ON baseline is not fitted properly.

The exact cause for the voltage shift of the Q_γ-V plot is not known. One possibility is that, on repolarization, Q_γ requires some finite time to be restored to the normal resting state. Thus, a few seconds after repolarization, Q_γ could be in a temporary off state that is different from the normal resting state. The voltage distribution of Q_γ in that off state could follow a Boltzmann distribution shifted by a few millivolts from that for the normal resting state. Another possibility is that Q_γ is made up of two components, the primary one being activated by the depolarizing pulses and the secondary one activated by the additional depolarization caused by the binding of the released Ca^{2+} on the myoplasmic face of the tubular membrane. In other words, the primary component is consistent with the trigger hypothesis and the secondary component is consistent with the feedback hypothesis. With the secondary compo-

nent present, the value of $\overline{V}_\gamma$ is slightly more negative than that without. Thus, when Ca release is suppressed, for example by repetitive stimulation, a small shift of $\overline{V}_\gamma$ to a less negative potential can be observed.

If Q_γ is completely caused by Ca release, then some features of our results are difficult to explain. For example, depletion of Ca^{2+} in the SR should be more effective with 50 mM EGTA than with 20 mM in the end pool solution, but the shifts in the Q-V plots with both concentrations of EGTA are comparable (Table II). The only sensible conclusion that can accommodate all the results is that there is a genuine, steeply voltage-dependent component of charge that has been convincingly dissected out from the total charge with four independent methods (Hui and Chen, 1992). Part of this component can be activated by Ca feedback, but that part is considered as secondary. Under normal conditions I_γ is manifested as a hump in some potential range, but its waveform can be broadened when the fiber is stimulated repeatedly at a relatively high rate. Although Q_γ, serving as a voltage sensor, is not suppressed during repetitive stimulation, Ca release can be substantially reduced due to a depletion of releasable Ca in the SR.

This project was supported by grants from the National Institutes of Health (NS-21955) and the Muscular Dystrophy Association. C. S. Hui was a recipient of a Research Career Development Award (NS-00976) from the NIH and W. Chen was a recipient of a postdoctoral fellowship from the Indiana Heart Association.

Original version received 29 April 1991 and accepted version received 23 January 1992.

REFERENCES

Adrian, R. H., and W. Almers. 1976. Charge movement in the membrane of striated muscle. *Journal of Physiology.* 254:339–360.

Adrian, R. H., W. K. Chandler, and R. F. Rakowski. 1976. Charge movement and mechanical repriming in skeletal muscle. *Journal of Physiology.* 254:361–388.

Adrian, R. H., and A. R. Peres. 1979. Charge movement and membrane capacity in frog muscle. *Journal of Physiology.* 289:83–97.

Almers, W. 1978. Gating currents and charge movements in excitable membranes. *Review of Physiology and Biochemical Pharmacology.* 82:96–190.

Brum, G., and E. Eios. 1987. Intramembrane charge movement in frog skeletal muscle fibres: properties of charge 2. *Journal of Physiology.* 387:489–517.

Chandler, W. K., and C. S. Hui. 1990. Membrane capacitance in frog cut twitch fibers mounted in a double Vaseline-gap chamber. *Journal of General Physiology.* 96:225–256.

Chandler, W. K., R. F. Rakowski, and M. F. Schneider. 1976. A nonlinear voltage dependent charge movement in frog skeletal muscle. *Journal of Physiology.* 254:245–283.

Chen, W., and C. S. Hui. 1989. Effects of tetracaine and maintained depolarization on charge movement components in frog cut twitch fibers. *Biophysical Journal.* 55:239*a*. (Abstr.)

Chen, W., and C. S. Hui. 1991*a*. Existence of Q_γ in frog cut twitch fibers with little Q_β. *Biophysical Journal.* 59:503–507.

Chen, W., and C. S. Hui. 1991*b*. Differential blockage of charge movement components in frog cut twitch fibres by nifedipine. *Journal of Physiology.* 444:579–603.

Csernoch, L., I. Uribe, M. Rodriguez, G. Pizzaro, and E. Rios. 1989. Q_γ and Ca release flux in skeletal muscle fibers. *Biophysical Journal.* 55:88*a*. (Abstr.)

Garcia, J., G. Pizarro, E. Rios, and E. Stefani. 1990. Depletion of the SR reduces the delayed charge movement of frog skeletal muscle. *Biophysical Journal.* 57:341*a*. (Abstr.)

Hodgkin, A. L., and P. Horowicz. 1960. Potassium contractures in single muscle fibres. *Journal of Physiology.* 153:386–403.

Horowicz, P., and M. F. Schneider. 1981. Membrane charge movement in contracting and non-contracting skeletal muscle fibres. *Journal of Physiology.* 314:565–593.

Huang, C. L.-H. 1982. Pharmacological separation of charge movement components in frog skeletal muscle. *Journal of Physiology.* 324:375–387.

Hui, C. S. 1983*a*. Pharmacological studies of charge movement in frog skeletal muscle. *Journal of Physiology.* 337:509–529.

Hui, C. S. 1983*b*. Differential properties of two charge components in frog skeletal muscle. *Journal of Physiology.* 337:531–552.

Hui, C. S. 1990. D600 binding sites on voltage-sensors for excitation-contraction coupling in frog skeletal muscle are intracellular. *Journal of Muscle Research and Cell Motility.* 11:471–488.

Hui, C. S. 1991*a*. Comparison of charge movement components in intact and cut twitch fibers of the frog. Effects of stretch and temperature. *Journal of General Physiology.* 98:287–314.

Hui, C. S. 1991*b*. Factors affecting the appearance of the slow charge component in frog cut twitch fibers. *Journal of General Physiology.* 98:315–347.

Hui, C. S., and W. K. Chandler. 1990. Intramembranous charge movement in frog cut twitch fibers mounted in a double Vaseline-gap chamber. *Journal of General Physiology.* 96:257–297.

Hui, C. S., and W. K. Chandler. 1991. Comparison of Q_β and Q_γ charge movement in frog cut twitch fibers. *Journal of General Physiology.* 98:429–464.

Hui, C. S., and W. Chen. 1992. Separation of charge movement components in frog cut twitch fibers with tetracaine. Critical comparison with other methods. *Journal of General Physiology.* 99:985–1016.

Hui, C. S., and R. L. Milton. 1987. Suppression of charge movement in frog skeletal muscle by D600. *Journal of Muscle Research and Cell Motility.* 8:195–208.

Luttgau, H. C., and H. G. Glitsch. 1976. Membrane physiology of nerve and muscle fibres. *Fortschritte der Zoologie.* 24:1–132.

Rakowski, R. F. 1981. Immobilization of membrane charge in frog skeletal muscle by prolonged depolarization. *Journal of Physiology.* 317:129–148.

Rakowski, R. F., P. M. Best, and M. R. James-Kracke. 1985. Voltage dependence of membrane charge movement and calcium release in frog skeletal muscle fibres. *Journal of Muscle Research and Cell Motility.* 6:403–433.

Vergara, J., and C. Caputo. 1983. Effects of tetracaine on charge movements and calcium signals in frog skeletal muscle fibers. *Proceedings of the National Academy of Sciences, USA.* 80:1477–1481.